A new model for nonlinear acoustic waves in a non-uniform lattice of Helmholtz resonators

Jean-François Mercier, Bruno Lombard

PROCEEDINGS OF THE ROYAL SOCIETY A

rspa.royalsocietypublishing.org

Research

Article submitted to journal

Subject Areas:
acoustics, mathematical physics

Keywords:
nonlinear acoustics, solitons, Burgers equation, fractional derivatives, diffusive representation, Helmholtz resonators

Author for correspondence:
Jean-François Mercier
e-mail:
jean-francois.mercier@ensta-paristech.fr

A new model for nonlinear acoustic waves in a non-uniform lattice of Helmholtz resonators

Jean-François Mercier[1], Bruno Lombard[2]

[1] POEMS, CNRS-INRIA-ENSTA UMR 7231, 828 Boulevard des Maréchaux, 91762 Palaiseau, France,
[2] LMA, CNRS UPR 7051, Centrale Marseille, Aix-Marseille Univ, F-13402 Marseille Cedex 20, France

Propagation of high amplitude acoustic pulses is studied in a 1D waveguide, connected to a lattice of Helmholtz resonators. An homogenized model has been proposed by Sugimoto (J. Fluid. Mech., **244** (1992)), taking into account both the nonlinear wave propagation and various mechanisms of dissipation. This model is extended to take into account two important features: resonators of different strengths and back-scattering effects. The new model is derived and is proved to satisfy an energy balance principle. A numerical method is developed and a better agreement between numerical and experimental results is obtained.

Royal Society Publishing
Informing the science of the future

1. Introduction

We are concerned in the dynamics of nonlinear waves in lattices. This subject has stimulated researches in a wide range of areas, including the theory of solitons and the dynamics of discrete networks. Numerous studies have been led in electromagnetism and optics [1], and many physical phenomena have been highlighted, such as discrete breathers [2–4], chaotic phenomena [5,6], dynamical multistability [7–9] and solitons or solitary waves [10–12]. We focus more specifically on solitary waves, which have been first observed and studied for surface waves in shallow water [13]. The main feature of these waves is that they can propagate without change of shape and with a velocity depending of their amplitude [14]. They have been studied in many physical systems, as in fluid dynamics, optics or plasma physics.

For elastic waves, numerous works have highlighted the existence of solitary waves in microstructured solids [17], periodic structures such as lattices or crystals [18–20], elastic layers [21–23], layered structures coated by film of soft material [24], periodic chains of elastics beads [25–27] and uniform or inhomogeneous rods [28–30].

In this paper, we are primarily interested in the field of acoustics, and only a few works dealt with this case, although experimental observations of solitary waves have been made in the atmosphere [31–33] or in the ocean [34–36]. Such a lack is mainly explained by the fact that the intrinsic dispersion of acoustic equations is too low to compete with the nonlinear effects, preventing from the occurrence of solitons. To observe these waves, geometrical dispersion must be introduced. It has been the object of the works of Sugimoto and his co-authors [37–40], where the propagation of nonlinear waves was considered in a tube connected to an array of Helmholtz resonators (Fig. 1). A model incorporating both the nonlinear wave propagation in the tube and the nonlinear oscillations in the resonators has been proposed. Theoretical and experimental investigations have shown the existence of acoustic solitary waves [37].

Sugimoto considers that all the resonators are the same, which allows to use a simplifying homogenization process. The drawback of such a restriction is that the reflection of an incident wave by a defect (for instance, a resonator different from the others) can not be considered. In a same way, the case of resonators with random features can not be treated. However, the case of variable resonators is important when studying the influence of manufacturing defects or the influence of aging of the guiding device on wave propagation. As a remedy to Sugimoto's model failures, it is necessary to be able to consider resonators with different heights and it is the aim of this paper. The present study extends the work of Sugimoto and develops a more general model taking the geometry of the propagation medium into account, in a more realistic manner.

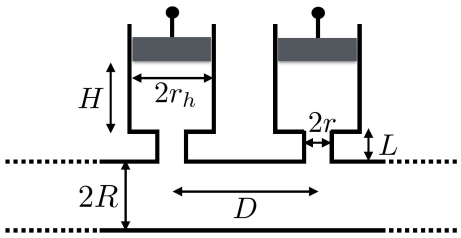

Figure 1. Sketch of the guide connected with Helmholtz resonators.

Let us recall briefly the Sugimoto model. In this original model, the wave fields are split into right-going waves (denoted +) and left-going waves (denoted -) that do not interact together during their propagation. In particular, no reflections by the resonators are assumed. The variables are the axial particle velocity of the gas $u^{\pm}$ and the associated excess pressure in the resonators $p^{\pm}$. The model involves two coupled equations for each simple wave: a nonlinear hyperbolic-parabolic PDE (Partial Differential Equation) describing the propagation of large

amplitude acoustic waves in the tube, and a nonlinear ODE (Ordinary Differential Equation) describing the oscillations in the Helmholtz resonators. The equations are very similar for the unknowns (u^+, p^+) (defined in Fig. 2) or (u^-, p^-) and they read [45] as two systems of two

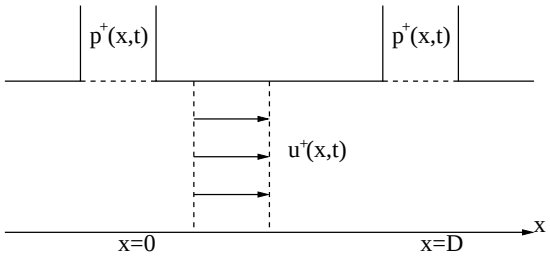

Figure 2. Unknowns for the right-going propagation in Sugimoto's model.

equations ($+$ or $-$):

$$\begin{cases} \dfrac{\partial u}{\partial t}^{\pm} + \dfrac{\partial}{\partial x}\left(\pm a u^{\pm} + b\dfrac{(u^{\pm})^2}{2}\right) \mp \bar{c}\dfrac{\partial^{-1/2}}{\partial t^{-1/2}}\dfrac{\partial u}{\partial x}^{\pm} - d\dfrac{\partial^2 u}{\partial x^2}^{\pm} = \mp\bar{e}\dfrac{\partial p}{\partial t}^{\pm}, & (1.1a) \\ \dfrac{\partial^2 p}{\partial t^2}^{\pm} + f\dfrac{\partial^{3/2} p}{\partial t^{3/2}}^{\pm} + g p^{\pm} - m\dfrac{\partial^2 (p^{\pm})^2}{\partial t^2} + n\left|\dfrac{\partial p}{\partial t}^{\pm}\right| \dfrac{\partial p}{\partial t}^{\pm} = \pm h u^{\pm}. & (1.1b) \end{cases}$$

The definition of the constants $a, b, \cdots$ will be recalled later. The viscothermal dissipative effects in the tube and in the throats of resonators are modeled by fractional integral and derivative [41], that amount to convolution products with singular kernels. The coupling between (1.1*a*) and (1.1*b*) is done by the coefficients e and h. If the resonators are suppressed, then the coefficient $e \to 0$: no coupling occurs, and the classical Chester's equation is recovered [42].

In some previous papers, we have proposed a time-domain numerical method to solve this model [43,44] and we have studied numerically and experimentally the propagation of high amplitude pulses in a lattice of Helmholtz resonators. The comparisons between numerical and experimental results have validated the theoretical model [43]. However, the model (1.1) has some shortcomings:

- it is based on an averaged description of the geometry, similar to an homogenized model, in which the resonators are approximated as continuously distributed. The advantage of such approach is to get equations with constant coefficients, suitable for theoretical analysis: in particular, they can be reduced to a Korteweg-de Vries equation [38,45]. But a drawback is that the propagation medium must be periodic, and thus it is restricted to resonators of the same height H. In the case of resonators of height varying slowly, this homogenized model might remain accurate but not in the case of an abrupt change of height. An additional disadvantage is that this homogenized model is valid only if $\lambda \gg D$, where λ is the typical size of the wave (*i.e.* the wavelength for a propagating wave or the spatial extent for a soliton) and D is the distance between two resonators.
- it considers only one-way propagations. Sugimoto supposed that no wave reflections by the resonators occur, arguing that this approximation is accurate if $V/AD \ll 1$ [38] where V is the volume of the resonators and A is the area of the main tube cross section.
- it is not adapted to perform an energy balance as soon as $c \neq 0$ [45].

In this paper, we improve the original Sugimoto's model (1.1), and the improvements are made in several ways. First we introduce a discrete description of the resonators by considering variable coefficients. A consequence is that the requirement of a long wavelength is no longer

necessary. Second, we allow the reflection of waves and we take into account the interaction of waves propagating in both directions. Finally, we modify the fractional integral in (1.1*a*), which leads to a formulation suitable for an energy balance. The new model we will establish in (2.30) is a single system coupling the three unknowns u^+, u^- and p:

$$\begin{cases} \dfrac{\partial u^+}{\partial t} + \dfrac{\partial}{\partial x}\left(au^+ + b\dfrac{(u^+)^2}{2}\right) + \dfrac{c(x)}{a}\dfrac{\partial^{1/2}u^+}{\partial t^{1/2}} - d\dfrac{\partial^2 u^+}{\partial x^2} = {}_e(x)(1-2mp)\dfrac{\partial p}{\partial t}, \\ \dfrac{\partial u^-}{\partial t} + \dfrac{\partial}{\partial x}\left(-au^- + b\dfrac{(u^-)^2}{2}\right) + \dfrac{c(x)}{a}\dfrac{\partial^{1/2}u^-}{\partial t^{1/2}} - d\dfrac{\partial^2 u^-}{\partial x^2} = e(x)(1-2mp)\dfrac{\partial p}{\partial t}, \\ \dfrac{\partial^2 p}{\partial t^2} + f\dfrac{\partial^{3/2}p}{\partial t^{3/2}} + g(x)p - m\dfrac{\partial^2(p^2)}{\partial t^2} + n(x)\left|\dfrac{\partial p}{\partial t}\right|\dfrac{\partial p}{\partial t} = h(x)(u^+ - u^-). \end{cases}$$

The paper is organized as follows. In section 2, the general equations in the tube and in the resonators are given and the new model (2.30) is derived. Moreover, comparison with the Sugimoto model are proposed. In section 3, we derive a first-order formulation (3.6) of the new model, for two purposes: to determine an energy balance and also to build a numerical scheme. In section 4, numerical results are presented to validate and to show the improvements related with the new model.

2. The new model

In this section, we will establish the new model (2.30), improving Sugimoto's model (1.1) [38]. The improvements will be added sequentially: first the extension to counterpropagating waves and to a local description of the geometry. Then the links with the original model, using a one-way approximation and an homogenized description, will be precised. Last, a modification of the fractional integral will be introduced. Notably, thanks to the last step, we will be able to derive an energy balance for the new model.

The configuration under study is made up of an air-filled tube connected with uniformly distributed cylindrical Helmholtz resonators (see Fig. 1). The geometrical parameters are the radius of the guide R, the axial spacing between successive resonators D, the radius of the neck r, the length of the neck L, the radius of the cavity r_h and the height of the cavity H, which can vary from one resonator to the other. The cross-sectional area of the guide is $A = \pi R^2$ and that of the neck is $B = \pi r^2$, the volume of each resonator is $V = \pi r_h^2 H$.

The unknows are the velocity of the right-going wave u^+, the velocity of the left-going wave u^- and p the total excess pressure in the resonators, induced by both waves. As it will be detailed later, p is not simply $p^+ + p^-$ where $p^\pm$ are solutions of (1.1).

(a) Equation in the tube

(i) General equations

In this part we recall briefly the general equations governing the nonlinear acoustic waves in the tube [38]. The physical parameters are the ratio of specific heats at constant pressure and volume γ; the pressure at equilibrium p_0; the density at equilibrium ρ_0; the Prandtl number Pr; the kinematic viscosity ν; and the ratio of shear and bulk viscosities μ_v/μ. The linear sound speed a_0 and the sound diffusivity ν_d are defined by

$$a_0 = \sqrt{\frac{\gamma p_0}{\rho_0}}, \qquad \nu_d = \nu\left(\frac{4}{3} + \frac{\mu_v}{\mu} + \frac{\gamma - 1}{\mathrm{Pr}}\right). \tag{2.1}$$

Starting from the compressible Navier-Stokes equations, Sugimoto [38] obtained the following nonlinear equation for the horizontal velocities $u^\pm$:

$$\frac{\partial u^\pm}{\partial t} + \left(\pm a + bu^\pm\right)\frac{\partial u^\pm}{\partial x} = \pm\frac{a_0}{2\rho_0}F^\pm + d\frac{\partial^2 u^\pm}{\partial x^2}, \tag{2.2}$$

with

$$F^{\pm}(x) = \frac{1}{A}\int_{\sigma(x)} (\rho v_n^{\pm})(x, y(s), z(s))ds, \tag{2.3}$$

and

$$a = a_0, \quad b = \frac{\gamma+1}{2}, \quad d = \frac{\nu_d}{2}. \tag{2.4}$$

In Eq. 2.2, $u^{\pm}$ represent mean axial velocities over the cross section of the tube. Eq. 2.2 is obtained after restriction to unidirectional propagation, and under the assumption of weak nonlinearities, which allow to use Riemann invariants along the characteristics, noted with the $\pm$ subscript according to the way of propagation. $\sigma(x)$ is a path along the boundary of a cross section of the tube and s is the curvilinear abscissa (see Fig. 3). The diffusivity of sound in the tube is introduced by the coefficient d. $F^{\pm}$ is the mean mass flux at position x, with $v_n^{\pm}$ the small deviation of the component of the velocity normal inward to the inner surface of the tube ($v_n^{\pm}$ lies in the $y-z$ plane and is also precised on Fig. 4). The integral is taken along the periphery of the cross-section at x (see Fig. 3). $F^{\pm}$ is due to the coupling between the main flow $u^{\pm}$ and two areas, represented in grey on Fig. 4. More precisely, $F^{\pm}$ takes into account:

- the connections of the main tube with the resonators,
- the wall friction due to the presence of a viscous boundary layer on the boundary of the tube.

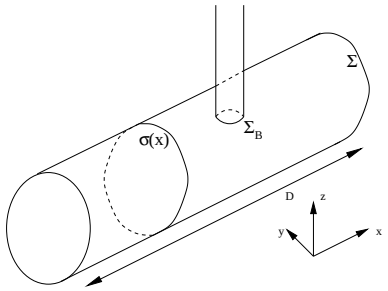

Figure 3. Perspective view of the tube. The unit portion Σ of the tube is connected to one resonator through the surface Σ_B. σ is the boundary of a cross section of the tube.

To precise the definition of $F^{\pm}$, we need to introduce some notations. We note Σ a part of length D (thus connected to only one resonator) of the tube, represented in Fig. 3. We note Σ_B the part of Σ connected to the cylindrical resonator, of area B. For simplicity, we approximate the junction between a resonator and the main tube as a disc, the real shape (intersection of two perpendicular tubes of different diameters) being more complicated. Sugimoto [38] obtained that:

$$\begin{aligned} \rho v_n^{\pm} &= -Q \quad \text{on} \quad \Sigma_B, \\ &= \rho_0 v_b^{\pm} \quad \text{on} \quad \Sigma \backslash \Sigma_B, \end{aligned} \tag{2.5}$$

with

$$\begin{aligned} Q &= \frac{V}{a_0^2 B}(1-2mp)\frac{\partial p}{\partial t}, \\ v_b^{\pm} &= C\sqrt{\nu}\frac{\partial^{-1/2}}{\partial t^{-1/2}}\frac{\partial u}{\partial x}^{\pm}, \end{aligned} \tag{2.6}$$

where

$$m = \frac{\gamma-1}{2\gamma p_0}. \tag{2.7}$$

This coefficient m describes the adiabatic process in the cavity up to the second-order nonlinearity. Q is the mass flux density over B into the resonator cavity (see Fig. 4). $v_b^{\pm}$ corresponds to

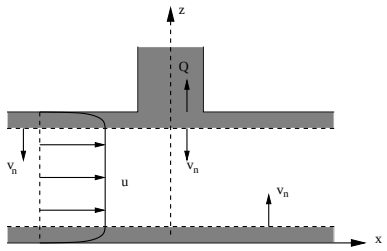

Figure 4. Definition of $v_n^{\pm}$. In grey is represented the viscous boundary layer and the inside of the resonators. $v_n^{\pm}$ is defined on the boundary of this gray area.

viscothermal losses in the boundary layer of the tube [46], modeled by a fractional operator of order -1/2, proportional to $1/(i\,\omega)^{1/2}$ in the frequency domain, with C the dissipation in the boundary layer:

$$C = 1 + \frac{\gamma - 1}{\sqrt{\mathrm{Pr}}}.$$

The Riemann-Liouville fractional integral of order $1/2$ of a causal function $w(t)$ is defined by

$$\frac{\partial^{-1/2}}{\partial t^{-1/2}} w(t) = \frac{H(t)}{\sqrt{\pi\, t}} * w = \frac{1}{\sqrt{\pi}} \int_0^t (t-\tau)^{-1/2} w(\tau)\, d\tau, \tag{2.8}$$

where * is the convolution product in time, and $H(t)$ is the Heaviside step function [47].

(ii) Determination of the flux $F^{\pm}$

In this part, we determine explicitly the flux $F^{\pm}$ at each position x. These results are new since, as we will detail later, Sugimoto only considered the spatial average of $F^{\pm}$. For convenience, Σ is located in $x \in]-r, D-r[$, the part Σ_B being then centered at $x = 0$, located in $x \in]-r, r[$ (see Fig. 5). Then we can determine $F^{\pm}$ at each position x:

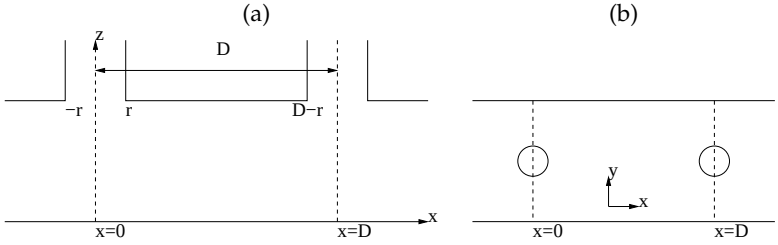

Figure 5. Portion of length D of the tube. View from the side (a). View from above (b).

- For $x \in]r, D-r[$: then $\sigma(x)$ is a disc of radius R and $\rho v_n^{\pm} = \rho_0 v_b^{\pm}$ on σ. Therefore

$$\begin{aligned} F^{\pm}(x) &= \frac{1}{A} \int_0^{2\pi} (\rho v_n^{\pm})(x, R\sin\theta, R\cos\theta) R d\theta, \\ &= \frac{1}{A} (2\pi R)\, \rho_0 v_b^{\pm}, \end{aligned}$$

  where θ is measured with respect to the z axis (as α in Fig. 6(a)).

• For $x \in]-r, r[$: on Fig. 6(a) is represented a cross section of the tube for $x \in]-r, r[$. The

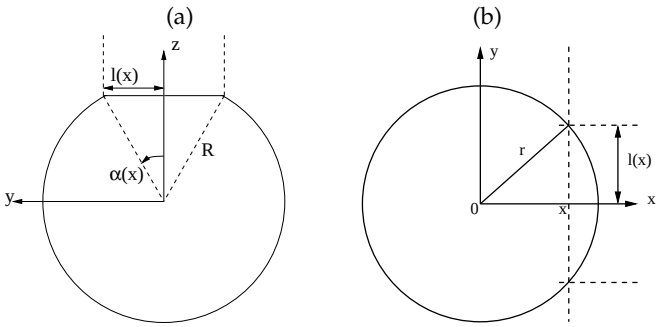

Figure 6. (a) $\sigma(x)$ for $x \in]-r, r[$; (b) view from above of the resonators in $x \in]-r, r[$.

integration path $\sigma(x)$ is made of two parts: (i) a line of length $2\ell(x)$ on which $\rho v_n^{\pm} = -Q$; (ii) a portion of a circle of radius R, between the angles $\theta = \alpha$ and $\theta = 2\pi - \alpha$, on which $\rho v_n^{\pm} = \rho_0 v_b^{\pm}$. Using Fig. 6(b) representing Σ_B seen from above, it is straightforward to find that:

$$\ell(x) = \begin{cases} 0 & \text{for} \quad x \in]r, D-r[, \\ \sqrt{r^2 - x^2} & \text{for} \quad x \in]-r, r[. \end{cases} \tag{2.9}$$

Using Fig. 6(a), one finds also that $\alpha(x) = \arcsin\left(\ell(x)/R\right)$.

Then Eq. (2.3) becomes:

$$\begin{aligned} F^{\pm}(x) &= \frac{1}{A}\left[\int_{\alpha(x)}^{2\pi-\alpha(x)} (\rho_0 v_b^{\pm})(x, R\sin\theta, R\cos\theta) R d\theta + \int_{-\ell(x)}^{\ell(x)} (-Q) ds\right], \\ &= \frac{2}{A}\left\{[\pi - \alpha(x)]\, R\rho_0 v_b^{\pm} - Q\ell(x)\right\}. \end{aligned}$$

To sum up, using the values of Q and $v_b^{\pm}$ from Eq. (2.6), one deduces that for all $x \in]-r, D-r[$:

$$\frac{a_0}{2\rho_0} F^{\pm} = c(x) \frac{\partial^{-1/2}}{\partial t^{-1/2}} \frac{\partial u}{\partial x}^{\pm} - e(x)(1 - 2mp)\frac{\partial p}{\partial t}, \tag{2.10}$$

where we have introduced the functions

$$\begin{cases} c(x) &= c_0\left[1 - \dfrac{1}{\pi}\arcsin\left(\dfrac{\ell(x)}{R}\right)\right], \\ e(x) &= e_0\ell(x), \end{cases} \tag{2.11}$$

with the coefficients

$$c_0 = \frac{C\, a_0\sqrt{\nu}}{R}, \quad e_0 = \frac{V}{\rho_0\, a_0\, AB}, \tag{2.12}$$

ans V is the volume of the resonator at $x = 0$. This result has been obtained for a unit part of the tube located in $x \in]-r, D-r[$. Now we consider the entire tube, in which the resonators are centered at $x = iD$, $i = 1, 2, \cdots$ (see Fig. 7). We note V_i the volume (and H_i the height) of the i-th resonator, located at $x_i = iD$. In the i-th cell $x \in [x_i - D/2, x_i + D/2]$, represented in grey on Fig.

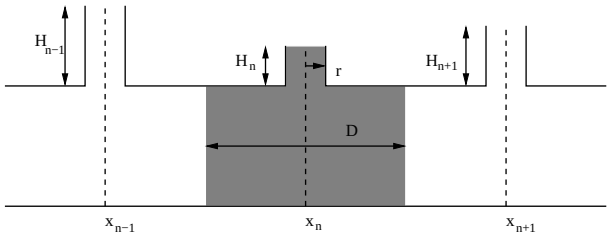

Figure 7. Side view of the guide connected to Helmholtz resonators. The i-th cell is highlighted in grey.

7, Eq. (2.2) takes the form

$$\frac{\partial u^{\pm}}{\partial t}+\frac{\partial}{\partial x}\left(\pm a u^{\pm}+b\frac{(u^{\pm})^2}{2}\right)\mp c(x)\frac{\partial^{-1/2}}{\partial t^{-1/2}}\frac{\partial u^{\pm}}{\partial x}-d\frac{\partial^2 u^{\pm}}{\partial x^2}=\mp e(x)(1-2mp)\frac{\partial p}{\partial t}, \tag{2.13}$$

with $c(x)$ and $e(x)$ defined by

$$\left\{\begin{array}{lcl} c(x) & = & c_0\left[1-\frac{1}{\pi}\arcsin\left(\frac{\ell_i(x)}{R}\right)\right], \\ e(x) & = & e_i\ell_i(x), \end{array}\right. \tag{2.14}$$

where

$$\ell_i(x)=\left\{\begin{array}{ll} 0 & \text{for} \quad r<|x-x_i|\leq\frac{D}{2}, \\ \sqrt{r^2-(x-x_i)^2} & \text{for} \quad |x-x_i|\leq r, \end{array}\right. \tag{2.15}$$

with c_0 defined in (2.12) and

$$e_i=\frac{V_i}{\rho_0\, a_0\, AB}. \tag{2.16}$$

(b) Equation in the resonators

To model the air oscillation in the neck of identical resonators, Sugimoto established the following equation for the excess pressure p in a resonator of volume V [48,49]:

$$\frac{\partial^2 p}{\partial t^2}+f\frac{\partial^{3/2} p}{\partial t^{3/2}}+gp-m\frac{\partial^2 p^2}{\partial t^2}+n\left|\frac{\partial p}{\partial t}\right|\frac{\partial p}{\partial t}=gp', \tag{2.17}$$

with

$$f=\frac{2\sqrt{\nu}}{r}\frac{L'}{L_e}, \quad g=\omega_e^2=\frac{a_0^2 B}{L_e V}, \quad n=\frac{V}{B\, L_e\, \rho_0\, a_0^2}. \tag{2.18}$$

The coefficients m (2.7) and n describe nonlinear processes in the resonators. The semi-empirical coefficient n accounts for the jet loss resulting from the difference in inflow and outflow patterns [38,40]. As it has been illustrated [43], these nonlinear processes have to be included to get a good agreement with the experimental measurements. The Caputo fractional derivative of order 3/2 is obtained by applying (2.8) to $\partial^2 p/\partial t^2$. Corrected lengths have been introduced: $L'=L+2\,r$ accounts for the viscous end corrections, and the corrected length $L_e=L+\eta$ accounts for the end corrections at both ends of the neck, where $\eta\approx 0.82\,r$ is determined experimentally [38].

p' is the excess pressure at the mouth of the tube, exciting the excess pressure p in the resonators (see Fig. 8). To link p' to the main unknowns of the problem, Sugimoto used a linear approximation: to the right-going wave u^+, he associated the pressure $p'^+=(\gamma p_0/a_0)u^+$. In a symmetric way, $p'^-=-(\gamma p_0/a_0)u^-$ is associated to the left-going waves. In our configuration, p' is induced by both the right-going waves and the left-going waves and we suppose that we have

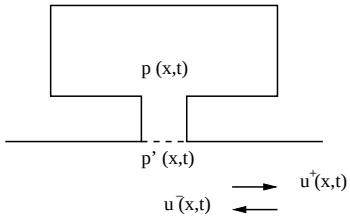

Figure 8. Excess pressure p in a resonator and excess pressure p' in the main tube, associated to the superposition of the right-going wave u^+ and the left-going wave u^-.

linearity: $p' = p'^+ + p'^-$. Therefore, it yields to

$$p' = (\gamma p_0/a_0)(u^+ - u^-). \tag{2.19}$$

Injecting (2.19) in (2.17) leads to

$$\frac{\partial^2 p}{\partial t^2} + f\frac{\partial^{3/2} p}{\partial t^{3/2}} + gp - m\frac{\partial^2 p^2}{\partial t^2} + n\left|\frac{\partial p}{\partial t}\right|\frac{\partial p}{\partial t} = h(u^+ - u^-), \tag{2.20}$$

with $h = \omega_e^2(\gamma\, p_0/a_0)$.

The extension of (2.17) to resonators of variable volume is easy since the coefficients g, h and n are constant in each resonator. It becomes for $|x - x_i| \leq r$, $i = 1, 2, \cdots$

$$\frac{\partial^2 p}{\partial t^2} + f\frac{\partial^{3/2} p}{\partial t^{3/2}} + g(x)p - m\frac{\partial^2 p^2}{\partial t^2} + n(x)\left|\frac{\partial p}{\partial t}\right|\frac{\partial p}{\partial t} = h(x)(u^+ - u^-), \tag{2.21}$$

with

$$g(x) = \frac{a_0^2 B}{L_e\, V_i}, \quad n(x) = \frac{V_i}{B\, L_e\, \rho_0\, a_0^2}, \quad h(x) = \frac{\gamma\, p_0}{a_0} g(x). \tag{2.22}$$

The functions $g(x)$, $h(x)$ and $n(x)$ depend on x because the resonators have different heights, but they are constant on each resonator. More precisely, they just depend on n, the index of the resonator. Note that (2.21) is not solved outside the resonators (that is on $r < |x - x_i| \leq \frac{D}{2}$) contrary to (1.1*b*). Note also that the model (2.13)-(2.21) could be easily extended to the case of resonators not periodically placed (only the values of x_i would have to be changed).

(c) Comparison with Sugimoto's model

To sum up the two previous paragraphs, we are led to solve the three coupled equations:

$$\begin{cases} \dfrac{\partial u^\pm}{\partial t} + \dfrac{\partial}{\partial x}\left(\pm a u^\pm + b\dfrac{(u^\pm)^2}{2}\right) & (2.23a) \\[2ex] \mp c(x)\dfrac{\partial^{-1/2}}{\partial t^{-1/2}}\dfrac{\partial u^\pm}{\partial x} - d\dfrac{\partial^2 u^\pm}{\partial x^2} = \mp e(x)(1 - 2mp)\dfrac{\partial p}{\partial t}, & (2.23b) \\[2ex] \dfrac{\partial^2 p}{\partial t^2} + f\dfrac{\partial^{3/2} p}{\partial t^{3/2}} + g(x)p - m\dfrac{\partial^2 p^2}{\partial t^2} + n(x)\left|\dfrac{\partial p}{\partial t}\right|\dfrac{\partial p}{\partial t} = h(x)(u^+ - u^-). & (2.23c) \end{cases}$$

In this paragraph, we show that the original model (1.1) of Sugimoto can be recovered from the new model (2.23). In this aim, we have to introduce two ingredients:

- a restriction to only one-way propagations: for right-going waves ($u^- = 0$), we note p^+ the associated pressure p and for left-going waves ($u^+ = 0$), we note p^- the pressure p,

- an averaged description of the geometry: to derive a model with constant coefficients, Sugimoto used identical resonators of volume V and he introduced a continuous approximation of the tube geometry and he used a mean value of the flux,

$$\bar{F}^{\pm} = \frac{1}{D}\int_{x=0}^{D} F^{\pm}(x)dx. \tag{2.24}$$

This corresponds to taking in (2.23*a*)-(2.23*b*) the mean values of $c(x)$ and $e(x)$. Using (2.11) and (2.12) is deduced

$$\bar{e} = \frac{1}{D}\int_{x=0}^{D} e(x)dx = e_0\frac{B}{2D} = \frac{V}{2\,\rho_0\,a_0\,A\,D}. \tag{2.25}$$

Also, thanks to the approximation for $R \gg r$:

$$\arcsin\left(\frac{\sqrt{r^2-x^2}}{R}\right) \simeq \frac{\sqrt{r^2-x^2}}{R}, \tag{2.26}$$

and using (2.11) and (2.12), we get:

$$\bar{c} = \frac{1}{D}\int_{x=0}^{D} c(x)dx = c_0\left(1-\frac{r^2}{2RD}\right) = C\,a_0\sqrt{\nu}\left(\frac{1}{R}-\frac{B}{2AD}\right) = C\,a_0\sqrt{\nu}\frac{1}{R^*}, \tag{2.27}$$

with

$$\frac{1}{R^*} = \frac{1}{R} - \frac{B}{2AD}, \tag{2.28}$$

where R^* is already used in [38]. Using these two ingredients, (2.23) degenerates in two families of two coupled equations:

$$\begin{cases} \dfrac{\partial u}{\partial t}^{\pm} + \dfrac{\partial}{\partial x}\left(\pm a u^{\pm} + b\dfrac{(u^{\pm})^2}{2}\right) \mp \bar{c}\dfrac{\partial^{-1/2}}{\partial t^{-1/2}}\dfrac{\partial u}{\partial x}^{\pm} - d\dfrac{\partial^2 u}{\partial x^2}^{\pm} = \mp\bar{e}(1-2mp^{\pm})\dfrac{\partial p}{\partial t}^{\pm} & (2.29a) \\ \dfrac{\partial^2 p}{\partial t^2}^{\pm} + f\dfrac{\partial^{3/2} p}{\partial t^{3/2}}^{\pm} + gp^{\pm} - m\dfrac{\partial^2 (p^{\pm})^2}{\partial t^2} + n\left|\dfrac{\partial p}{\partial t}^{\pm}\right|\dfrac{\partial p}{\partial t}^{\pm} = \pm h u^{\pm}. & (2.29b) \end{cases}$$

(2.29) is not exactly (1.1): in the original model, Sugimoto neglected the term $2mp^{\pm}$ in the right-hand-side of (1.1*a*). As we will see later, this term prevents from establishing an energy balance and this may explain why Sugimoto didn't consider this term.

(d) Elimination of the fractional integral

The final step in this section is to modify slightly the model (2.23) to get what we will call the new model (2.30). This one satisfies an energy balance, which is a key ingredient for proving its well-posedness. On the contrary, starting from (2.23*a*)-(2.23*b*) (or even from (1.1*a*)), an energy balance can be obtained only if $c = 0$, as done in [45]. To derive an energy balance in the case $c \neq 0$, we will determine (2.30), an alternate form of (2.23*a*)-(2.23*b*) with no fractional integral. This derivation is based on the first order approximation

$$\frac{\partial u}{\partial t}^{\pm} \simeq \pm a\frac{\partial u^{\pm}}{\partial x}.$$

Injecting this in (2.23*a*)-(2.23*b*) leads to the new model we will consider in the rest of the paper:

$$\begin{cases} \dfrac{\partial u}{\partial t}^{\pm} + \dfrac{\partial}{\partial x}\left(\pm a u^{\pm} + b\dfrac{(u^{\pm})^2}{2}\right) + \dfrac{c(x)}{a}\dfrac{\partial^{1/2} u^{\pm}}{\partial t^{1/2}} - d\dfrac{\partial^2 u}{\partial x^2}^{\pm} = \mp e(x)(1-2mp)\dfrac{\partial p}{\partial t}, & (2.30a) \\ \dfrac{\partial^2 p}{\partial t^2} + f\dfrac{\partial^{3/2} p}{\partial t^{3/2}} + g(x)p - m\dfrac{\partial^2 (p^2)}{\partial t^2} + n(x)\left|\dfrac{\partial p}{\partial t}\right|\dfrac{\partial p}{\partial t} = h(x)(u^+ - u^-). & (2.30b) \end{cases}$$

The rigorous derivation is detailed in Appendix B.

Before considering the numerical discretization of (2.30), let us emphasize that, compared to Sugimoto's model, the new model (2.30) incorporates three improvements: first it considers a two-way propagation; second it takes into account the precise geometry of the tube and the possibility of resonators with different heights, through the varying coefficients $c(x)$, $e(x)$, $g(x)$, $h(x)$ and $n(x)$; third and last it replaces $\dfrac{\partial^{-1/2}}{\partial t^{-1/2}}\dfrac{\partial}{\partial x}$ by $\dfrac{\partial^{1/2}}{\partial t^{1/2}}$, leading to a system suitable to establish an energy balance.

3. First-order system

In this section and in the rest of the paper, we focus on the new model (2.30) derived in the previous section and we exploit it, analytically and numerically. We write it in the form (3.6), suitable for a numerical discretization and to establish an energy balance. First we give explicit expressions of the fractional derivatives by approximating them by diffusive representations. Then we will define an energy associated to (2.30) and show that it decreases. Last we will also derive a particular first-order form of (2.30), suitable for a numerical treatment and we will present the numerical scheme to solve this system.

(a) Diffusive approximation

The fractional integral (2.8) is nonlocal in time and relies on the full history of $w(t)$, which is numerically memory-consuming. An alternative approach is based on a diffusive representation of fractional derivatives, and then on its approximation. This method has already been presented in [43,44] and we just recall it briefly:

$$\frac{\partial^{-1/2}}{\partial t^{-1/2}} w(t) \simeq \sum_{\ell=1}^{N} \mu_\ell \, \varphi_\ell(t), \tag{3.1}$$

where the diffusive variables $\varphi_\ell(t) = \varphi(t, \theta_\ell)$ satisfy the ODE

$$\begin{cases} \dfrac{\partial \varphi_\ell}{\partial t} = -\theta_\ell^2 \, \varphi_\ell + \dfrac{2}{\pi} \, w, \\ \varphi_\ell(0) = 0. \end{cases} \tag{3.2}$$

(3.1) follows from a quadrature formula on N points, with weights μ_ℓ and nodes θ_ℓ, which are determined by an optimization process.

To get fractional derivatives, we derivate (3.1). Then we deduce:

$$\frac{\partial^{1/2} w}{\partial t^{1/2}} = \frac{\partial}{\partial t}\frac{\partial^{-1/2} w}{\partial t^{-1/2}} \simeq \sum_{\ell=1}^{N} \mu_\ell \, \frac{\partial \varphi_\ell}{\partial t}(t) = \mu_\ell \left(-\theta_\ell^2 \, \varphi_\ell + \frac{2}{\pi} \, w \right). \tag{3.3}$$

Similarly, the derivative of order $3/2$ is written

$$\frac{\partial^{3/2} w}{\partial t^{3/2}} = \frac{\partial}{\partial t}\frac{\partial^{1/2} w}{\partial t^{1/2}} \simeq \sum_{\ell=1}^{N} \mu_\ell \, \frac{\partial \xi_\ell}{\partial t}(t), \tag{3.4}$$

where we have introduced $\xi_\ell = d\varphi_\ell/dt$. If $w(0) = 0$, as it will be the case in the following, the diffusive variable $\xi_\ell(t)$ satisfies the following ODE (derivative of (3.2))

$$\begin{cases} \dfrac{\partial \xi_\ell}{\partial t} = -\theta_\ell^2 \, \xi_\ell + \dfrac{2}{\pi} \, \dfrac{\partial w}{\partial t}, \\ \xi_\ell(0) = 0. \end{cases} \tag{3.5}$$

Thanks to these diffusive approximations, (2.30) can be written as the following system

$$\left\{\begin{array}{ll}
\dfrac{\partial u^{\pm}}{\partial t}+\dfrac{\partial}{\partial x}\left(\pm a\,u^{\pm}+b\,\dfrac{(u^{\pm})^2}{2}\right) & (3.6a)\\
=-\dfrac{c}{a}\displaystyle\sum_{\ell=1}^{N}\mu_\ell\left(-\theta_\ell^2\,\varphi_\ell^{\pm}+\dfrac{2}{\pi}\,u^{\pm}\right)+d\,\dfrac{\partial^2 u^{\pm}}{\partial x^2}\mp e(1-2mp)\,q, & (3.6b)\\
\dfrac{\partial p}{\partial t}=q, & (3.6c)\\
\dfrac{\partial q}{\partial t}=h(u^{+}-u^{-})-g\,p-f\displaystyle\sum_{\ell=1}^{N}\mu_\ell\left(-\theta_\ell^2\,\xi_\ell+\dfrac{2}{\pi}\,q\right)+m\dfrac{\partial^2 p^2}{\partial t^2}-n\,|q|\,q, & (3.6d)\\
\dfrac{\partial \varphi_\ell^{\pm}}{\partial t}=-\theta_\ell^2\,\varphi_\ell^{\pm}+\dfrac{2}{\pi}\,u^{\pm}, \qquad \ell=1\cdots N, & (3.6e)\\
\dfrac{\partial \xi_\ell}{\partial t}=-\theta_\ell^2\,\xi_\ell+\dfrac{2}{\pi}\,q, \qquad \ell=1\cdots N. & (3.6f)
\end{array}\right.$$

(b) Energy balance

As already announced, the system (3.6)) is suitable to define an energy and to prove the energy decreasing, in an infinite medium and for smooth solutions:

Result 1. *We note*

$$\mathcal{E}=\mathcal{E}_1^{+}+\mathcal{E}_1^{-}+\mathcal{E}_2 \;\; \textit{and} \;\; \mathcal{K}=\mathcal{K}_1^{+}+\mathcal{K}_1^{-}+\mathcal{K}_2, \tag{3.7}$$

with

$$\left\{\begin{array}{ll}
\mathcal{E}_1^{\pm}=\dfrac{1}{2}\displaystyle\int_{\mathbb{R}}\left((u^{\pm})^2+\dfrac{\pi}{2}\,\dfrac{c}{a}\sum_{\ell=1}^{N}\mu_\ell\,\theta_\ell^2\,(\varphi_\ell^{\pm})^2\right)dx, & (3.8a)\\
\mathcal{E}_2=\dfrac{1}{2}\displaystyle\int_{\mathbb{R}}\left(\dfrac{eg}{h}p^2+\dfrac{e}{h}(1-2\,m\,p)\,q^2+\dfrac{\pi}{2}\,\dfrac{ef}{h}\sum_{\ell=1}^{N}\mu_\ell\,\theta_\ell^2\,\xi_\ell^2\right)dx, & (3.8b)\\
\mathcal{K}_1^{\pm}=\dfrac{\pi}{2}\displaystyle\int_{\mathbb{R}}\dfrac{c}{a}\sum_{\ell=1}^{N}\mu_\ell\left(\dfrac{\partial\varphi_\ell^{\pm}}{\partial t}\right)^2dx+\int_{\mathbb{R}}d\left(\dfrac{\partial u^{\pm}}{\partial x}\right)^2dx, & (3.8c)\\
\mathcal{K}_2=\displaystyle\int_{\mathbb{R}}\left(\dfrac{e\,n}{h}q^2\left(|q|-\dfrac{m}{n}q\right)+\dfrac{\pi}{2}\,\dfrac{e\,f}{h}\sum_{\ell=1}^{N}\mu_\ell\left(\dfrac{\partial\xi_\ell}{\partial t}\right)^2dx\right). & (3.8d)
\end{array}\right.$$

Neglecting the $2mp$ term in (2.30a), then we have the energy balance

$$\frac{d\mathcal{E}}{dt}=-\mathcal{K}. \tag{3.9}$$

The proof is reported in Appendix A. Let us mention three remarks on (3.9), justifying that $\mathcal{E}$ is a decreasing energy:

- The hypothesis $2mp\simeq 0$ in (2.30*a*) is consistent with Sugomoto's work, where only the influence of m in the resonators equation (1.1*b*) has been considered. It is also consistent with the hypothesis of a weak nonlinear regime. Indeed, we have justified that ([43,44]):

$$2mp^{\pm}\approx(\gamma-1)\,\frac{u^{\pm}}{a_0}, \tag{3.10}$$

  which is lower than 1 under the hypothesis of weak nonlinearity ($|u^{\pm}|\ll a_0$). We have not succeeded in obtaining a proof by taking the term $2mp$ into account in (2.30*a*).

- The term $\mathcal{E}$ in (3.7) is positive if $\mu_\ell > 0$ and $1 - 2mp > 0$. The first condition is imposed when the coefficients of the diffusive representation are determined during the optimisation process [43]. The second condition is satisfied in the weak nonlinear regime.
- The term $\mathcal{K}$ in (3.7) is positive if $\mu_\ell > 0$ and $m < n$. The first condition has been already discussed. The second condition reads $m/n = \frac{\gamma-1}{2}\frac{BL_e}{V} < 1$, where BL_e is the resonator neck volume, and V is the volume of the resonators. For the experimental configuration under study, this ratio is lower than 1 and thus the condition is satisfied.

(c) Numerical scheme

In this part, we present the numerical resolution of (3.6) with null initial conditions. A source term $s(t)$ at $x = 0$ models the acoustic source of a right-going wave: $u^+(0,t) = s(t)$, $u^-(0,t) = 0$. For numerical purpose, it is necessary to write the evolution equations as a first-order system in time. To do so, the term $\partial^2 p^2/\partial t^2$ in Eq. (3.6*d*) is expanded and leads to

$$(1-2mp)\frac{\partial q}{\partial t} = h(u^+ - u^-) - g\,p - f\sum_{\ell=1}^{N}\mu_\ell\left(-\theta_\ell^2\,\xi_\ell + \frac{2}{\pi}\,q\right) + 2mq^2 - n\,|q|\,q.$$

The $(4+3\,N)$ unknowns for the counter-propagating waves are gathered in the vector

$$\mathbf{U} = \left(u^+, u^-,\, p,\, q, \varphi_1^+, \cdots,\, \varphi_N^+, \varphi_1^-, \cdots,\, \varphi_N^-,\, \xi_1, \cdots,\, \xi_N\right)^T. \tag{3.11}$$

Then the nonlinear systems (3.6) is written in the form

$$\frac{\partial}{\partial t}\mathbf{U} + \frac{\partial}{\partial x}\mathbf{F}(\mathbf{U}) = \mathbf{G}\,\frac{\partial^2}{\partial x^2}\mathbf{U} + \mathbf{S}(\mathbf{U}), \tag{3.12}$$

where $\mathbf{F}$ is the flux function

$$\mathbf{F} = \left(au^+ + b\,\frac{(u^+)^2}{2}, -au^- + b\,\frac{(u^-)^2}{2},\, 0,\, 0, \cdots,\, 0\right)^T, \tag{3.13}$$

and where the source term $\mathbf{S}$ is

$$\mathbf{S} = \begin{pmatrix}
-\dfrac{c}{a}\displaystyle\sum_{\ell=1}^{N}\mu_\ell\left(-\theta_\ell^2\,\varphi_\ell^+ + \dfrac{2}{\pi}\,u^+\right) - e(1-2mp)\,q \\
-\dfrac{c}{a}\displaystyle\sum_{\ell=1}^{N}\mu_\ell\left(-\theta_\ell^2\,\varphi_\ell^- + \dfrac{2}{\pi}\,u^-\right) + e(1-2mp)\,q \\
q \\
\dfrac{1}{1-2mp}\left(h(u^+ - u^-) - g\,p - f\displaystyle\sum_{\ell=1}^{N}\mu_\ell\left(-\theta_\ell^2\,\xi_\ell + \dfrac{2}{\pi}\,q\right) + 2mq^2 - n\,|q|\,q\right) \\
-\theta_\ell^2\,\varphi_\ell^+ + \dfrac{2}{\pi}\,u^+, \qquad \ell = 1\cdots N \\
-\theta_\ell^2\,\varphi_\ell^- + \dfrac{2}{\pi}\,u^-, \qquad \ell = 1\cdots N \\
-\theta_\ell^2\,\xi_\ell + \dfrac{2}{\pi}\,q, \qquad \ell = 1\cdots N
\end{pmatrix}. \tag{3.14}$$

As soon as $m \neq 0$ and $n \neq 0$, $\mathbf{S}(\mathbf{U})$ is no longer a linear operator ($m = 0 = n$ has been considered in [44]). The Jacobian matrix $\frac{\partial \mathbf{F}}{\partial \mathbf{U}}$ in (3.13) is diagonalizable with real eigenvalues: $a + b\,u^+$, $-a + b\,u^-$ and 0 with multiplicity $3\,N + 2$, which ensures propagation with finite velocity. These eigenvalues do not depend on the quadrature coefficients μ_ℓ and θ_ℓ. The diagonal matrix $\mathbf{G} = \mathrm{diag}(d, d, 0, \cdots, 0)$ incorporates the volume attenuation.

Let us describe briefly the numerical procedure, details can be found in [43,44]. To compute the N quadrature coefficients μ_ℓ and θ_ℓ in (3.14), we use a nonlinear optimization with the positivity constraints $\mu_\ell \geq 0$ and $\theta_\ell \geq 0$ [43]. In order to integrate the system (3.12), a grid is introduced, with a uniform spatial mesh size Δx and a variable time step Δt_n. The computations are done with $N_x = 1000$ grid nodes. The approximation of the exact solution $\mathbf{U}(x_j = j\,\Delta\,x, t_n = t_{n-1} + \Delta t_n)$ is denoted by $\mathbf{U}_j^n$. A stability analysis [44] leads to the restriction on the time step

$$\beta = \frac{a_{\max}^{(n)} \Delta t_n}{\Delta x}\left(1 + \frac{1}{\mathrm{Pe}}\right) \leq 1. \tag{3.15}$$

$\mathrm{Pe} = a_{\max}^{(n)}\,\Delta x/2\,d$ is the discrete Péclet number, with $a_{\max}^{(n)} = a + b\,\max_j[\max(|u_j^{n+}|, |u_j^{n-}|)]$ the discrete velocity. $\mathrm{Pe} \approx 10^5$ in our configuration and in practice the generalized CFL number β is taken equal to 0.95. To treat the systems (3.12), a Strang splitting [51] is used, ensuring both simplicity and efficiency: the original equation (3.6) is split in a propagative equation and a forcing equation, which are solved successively with adequate time increments. The propagative part is solved by a standard second-order TVD scheme (a finite-volume scheme with flux limiters) for nonlinear hyperbolic PDE [52] combined with a centered finite-difference approximation [44].

4. Numerical experiments

In this section we illustrate numerically the improvements brought by the new model (2.30).

(a) Configuration

γ	p_0 (Pa)	ρ_0 (kg/m^3)	Pr	ν (m^2/s)	μ_v/μ
1.403	10^5	1.177	0.708	$1.57\,10^{-5}$	0.60
R (m)	D (m)	r (m)	L (m)	r_h (m)	H (m)
0.025	0.1	0.01	0.02	0.0215	0.07

Table 1. Physical parameters of the air at $15\,^\circ$C, and geometrical parameters of the tube with resonators.

The numerical experiments proposed along this section are based on the data of [43]. The reader is referred to this article for a complete description of the experimental setup. In summary, the explosion of a balloon at $x = 0$ (Fig. 9(a)) generates a shock wave, which propagates along a tube of length 6.15 m. This wave interacts with resonators regularly spaced from $x = 0.2$ m up to the end of the tube. A receiver is put at $x_r = 2.8$ m. The physical and geometrical parameters are given in table 1.

(b) Test 1: comparison with experiments

Fig. 9 (b-c) show comparisons between the models and the experiments [43]. Two heights are considered: $H = 7$ cm (b) and $H = 13$ cm (c). The signal is measured at $x_r = 2.8$ m for the source of Fig. 9 (a). For both models, a good agreement is observed between the simulated data and the experimental results. It is observed that higher resonators yield slower and larger solitary waves, as predicted by the theory [38].

The best agreement is obtained with the new model, especially for larger resonators heights. This is due to the fact that this new model takes into account a two-way propagation and variable coefficients. To illustrate this, we compare the velocity fields at $t = 0.012$ s on the spatial subdomain $[2,\ 4.5]$ m. Fig. 10 corresponds to the height of the resonators $H = 7$ cm whereas Fig. 11 corresponds to $H = 13$ cm. For the Sugimoto model (Fig. 10(a) and Fig. 11(a)), one-way propagation is assumed with constant coefficients so that only u^+ is determined. On the contrary, the new model (Fig. 10(b-c) and Fig. 11(b-c)) assume two-way propagations with

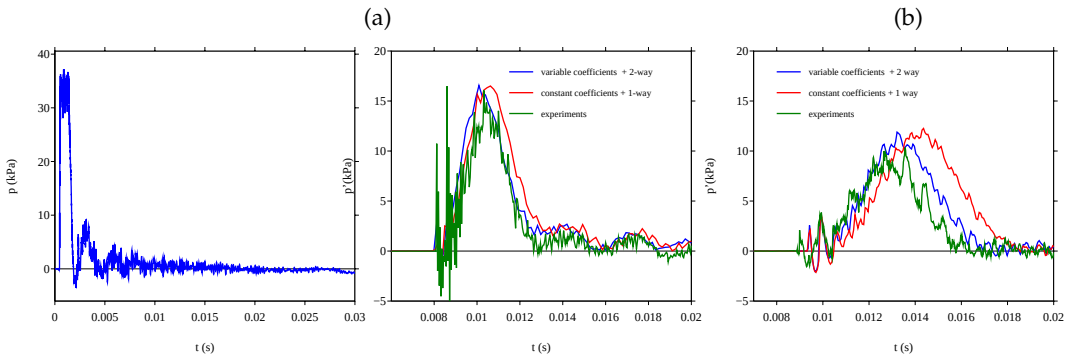

Figure 9. Time history of the excess pressure $p^{'}$ at $x = 0$ (a) and at the receiver at $x_r = 2.8$ m (b and c). Comparison between the models and the experiments. (b): $H = 7$ cm, (c): $H = 13$ cm.

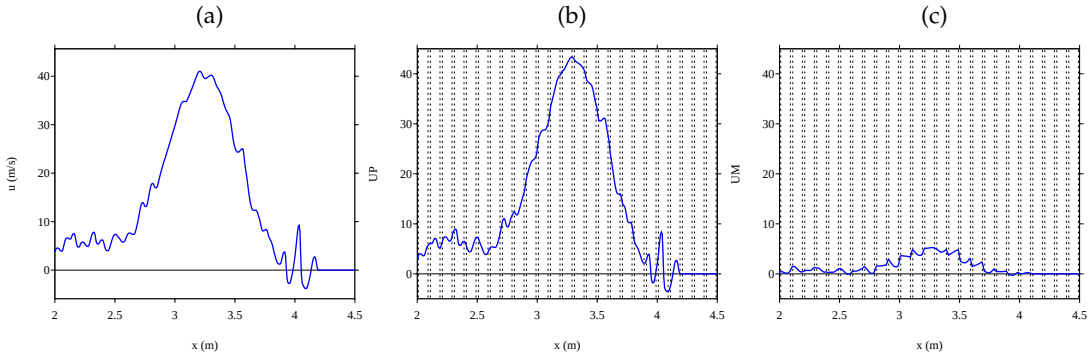

Figure 10. Snapshots of the fields for $H = 7$ cm at $t = 0.012$ s. (a) velocity $u = u^+$ from the Sugimoto model (one-way propagation with constant coefficients). For the new model (two-way propagation and variable coefficients), (b) u^+ and (c) u^-. The pairs of vertical dotted lines denote the resonators.

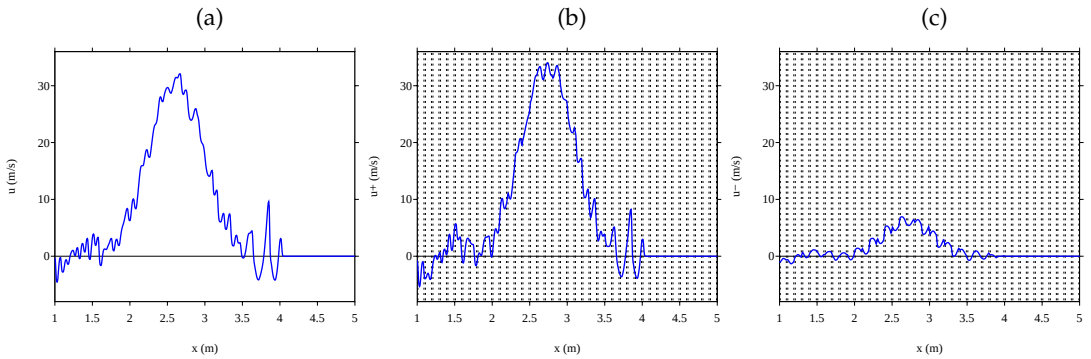

Figure 11. Snapshots of the fields for $H = 13$ cm at $t = 0.012$ s. (a) velocity $u = u^+$ from the Sugimoto model (one-way propagation with constant coefficients). For the new model (two-way propagation and variable coefficients), (b) u^+ and (c) u^-. The pairs of vertical dotted lines denote the resonators.

variable coefficients (3.6). The position of the resonators is denoted by a pair of vertical dotted lines, each one corresponding to the left and right extremities of the concerned resonator. For $H = 7$ cm, we obtain $|u^-| \ll |u^+|$ with $|u^+|/|u^-| \simeq 8$ and thus we are in a weak scattering regime.

This is why both models give similar results on Fig. 9(b). For $H = 13$ cm, the amplitude of $|u^-|$ is larger with $|u^+|/|u^-| \simeq 4$ which explains why Sugimoto's model is less accurate (Fig. 9(c)).

(c) Test 2: diffraction by a non-periodic configuration

To highlight the interest of the new model, we consider the case of a non-uniform distribution of Helmholtz resonators, which can be considered only thanks to the new model with variable coefficients.

(i) Diffraction by 3 defects

We consider the following configuration: the height of all the resonators is $H = 7$ cm, except around $x = 3$ m, where three resonators are 40 cm high. The variable coefficients $c(x)$ and $e(x)$ of (3.6), defined by (2.14), are sketched in Fig. 12. The coefficient c is independent of the height

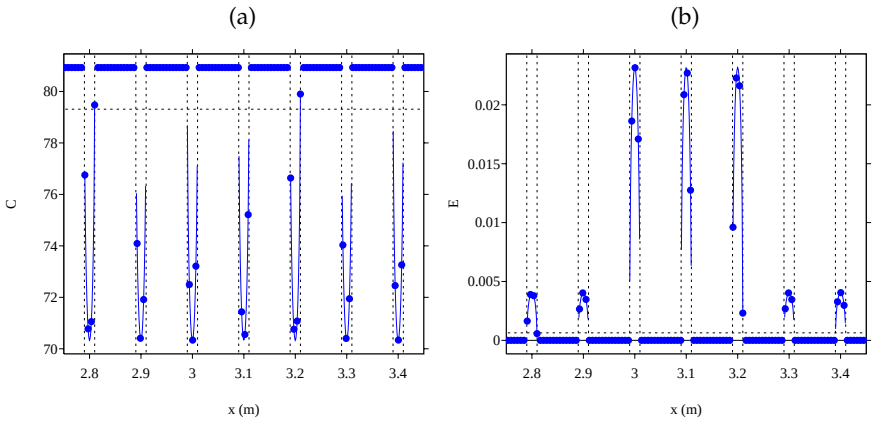

Figure 12. Spatial evolution of the coefficients around the defects at $x = 3$ m. The pairs of vertical dotted lines denote the extremities of the Helmholtz resonators. The horizontal dotted lines denote the mean value $\overline{c}$ and $\overline{e}$ of the coefficients. The solid blue lines represent the theoretical expressions, whereas the blue disks denote the discrete values used in the numerical code.

H, and has the non-null constant value c_0, defined in (2.12), outside the resonators (a). On the contrary, the coefficient e depends on H (see (2.12)), and is null outside the resonators (b). The horizontal dotted lines denote the mean value $\overline{c}$ and $\overline{e}$ of the coefficients, used in the model with constant coefficients and defined in (2.27) and in (2.25). The horizontal dotted lines denote the mean value $\overline{c}$ and $\overline{e}$ of the coefficients, used in the model with constant coefficients and defined in (2.27) and in (2.25). Due to the discretization, only 3 or 4 grid nodes lie inside each resonator. The effect of increasing the discretization will be studied in the next paragraph.

Fig. 13 presents snapshots of the excess pressure p' simulated by the new model. The positions of the modified resonators are sketched by vertical interfaces. At $t = 8.74$ ms, the solitary wave impacts the interface (a). At $t = 17.9$ ms, the simulations with and without the defects are compared. A reflected wave is clearly seen at the left of the interface when the defects are taken into account (b). It is seen that the transmitted solitary wave in presence of defects is deeply modified compared to the uniform case. Let us recall that the two ingredients of the new model are required to yield this reflection:

- variable coefficients to account for the difference of height H,
- 2-way propagation to account for the left-going wave.

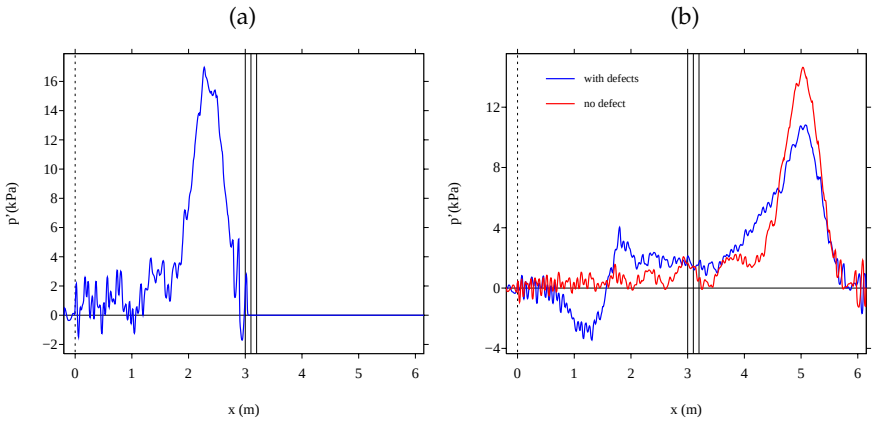

Figure 13. Snapshot of the simulated excess pressure $p^{'}$ at $t = 8.74$ ms (a) and $t = 17.9$ ms (b) with 3 defects. The vertical dotted line denotes the location of the source. The vertical solid lines denote the location of the defects. (a) at $t = 8.74$ ms, the solitary wave impacts the interface. (b) at $t = 17.9$ ms.

(ii) Influence of N_x

In the previous numerical experiments, the number of discretization points along the x-axis was $N_x = 1000$ which led to only 3 points in each resonator. We have checked that such discretization is enough to get a good solution, by comparing to the case $N_x = 2000$. This is shown on Fig. 14.

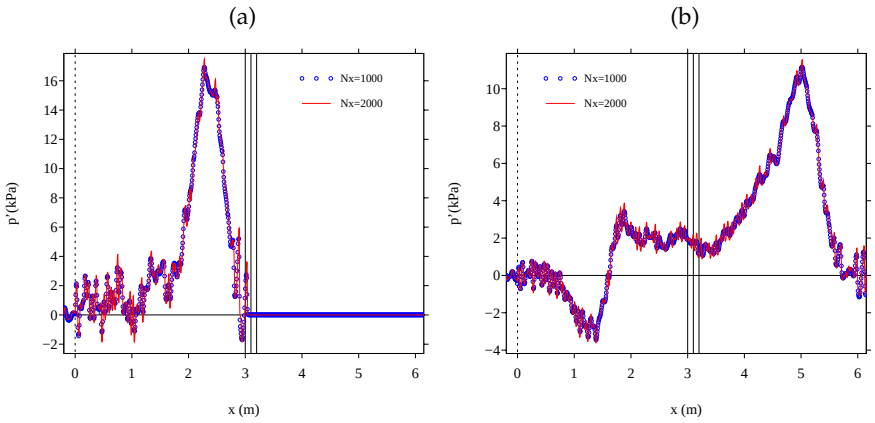

Figure 14. Snapshot of the simulated excess pressure $p^{'}$ at $t = 8.74$ ms (a) and $t = 17.9$ ms (b) with 3 defects and for $N_x = 1000$ and $N_x = 2000$.

5. Conclusion

The goal of this paper was to extend the results of the previous paper [43]. In [43], we have developed a numerical scheme to solve the equations governing the propagation of nonlinear waves in a tube connected to Helmholtz resonators. The model was restricted to identical resonators and to a one-way propagation. In this paper, we have extended the previous study to the case of variable resonators and to the presence of possible back-scattering of waves. The new model has been derived, starting from some local balance equations. It has been numerically validated by comparison with the previous model and with experiments. Better agreement with

experimental results has been obtained. Is has been also implemented in the case of the scattering by a defect, chosen as resonators with a locally different strength, such configuration creating a strong back-scattering. Propagation of nonlinear waves in random media [53] and comparisons with experimental data will be done in a near future.

Aknowledgement

The authors thank O. Richoux who gave access to his experimental measurements.

A. Energy decreasing

In this appendix is derived the following result for the energy decreasing.

Result 1: the energy $\mathcal{E} = \mathcal{E}_1^+ + \mathcal{E}_1^- + \mathcal{E}_2$ satisfies the energy balance $d\mathcal{E}/dt = -\mathcal{K}$ where $\mathcal{K} = \mathcal{K}_1^+ + \mathcal{K}_1^- + \mathcal{K}_2$ with $\mathcal{E}$ and $\mathcal{K}$ defined in (3.8).

Proof. The first step in to rewrite the system (3.6), eliminating the term $2m|p| \ll 1$ in (3.6*b*) and using (3.5), to get the the following system:

$$\begin{cases} \dfrac{\partial u^\pm}{\partial t} + \dfrac{\partial}{\partial x}\left(\pm a\, u^\pm + b\,\dfrac{(u^\pm)^2}{2}\right) = -\dfrac{c}{a}\displaystyle\sum_{\ell=1}^{N} \mu_\ell \dfrac{\partial \varphi_\ell^\pm}{\partial t} + d\,\dfrac{\partial^2 u^\pm}{\partial x^2} \mp e\, q, & \text{(A 1}a\text{)} \\ \dfrac{\partial p}{\partial t} = q, & \text{(A 1}b\text{)} \\ \dfrac{\partial q}{\partial t} = h(u^+ - u^-) - g\, p - f \displaystyle\sum_{\ell=1}^{N} \mu_\ell \dfrac{\partial \xi_\ell}{\partial t} + m\dfrac{\partial^2 p^2}{\partial t^2} - n\ |q|\ q, & \text{(A 1}c\text{)} \\ \dfrac{\partial \varphi_\ell^\pm}{\partial t} = -\theta_\ell^2\, \varphi_\ell^\pm + \dfrac{2}{\pi}\, u^\pm, \qquad \ell = 1 \cdots N, & \text{(A 1}d\text{)} \\ \dfrac{\partial \xi_\ell}{\partial t} = -\theta_\ell^2\, \xi_\ell + \dfrac{2}{\pi}\, q, \qquad \ell = 1 \cdots N. & \text{(A 1}e\text{)} \end{cases}$$

From (A 1*d*) is deduced

$$u^\pm = \frac{\pi}{2}\left(\frac{\partial \varphi_\ell^\pm}{\partial t} + \theta_\ell^2\, \varphi_\ell^\pm\right), \tag{A 2}$$

and from (A 1*e*) is deduced

$$q = \frac{\pi}{2}\left(\frac{\partial \xi_\ell}{\partial t} + \theta_\ell^2\, \xi_\ell\right). \tag{A 3}$$

In (A 1*c*), the derivative of p^2 is modified, using

$$\frac{\partial^2}{\partial t^2}(p^2)\, q = \frac{\partial}{\partial t}(p\, q^2) + q^3. \tag{A 4}$$

Such relation is easy to check by expanding both sides of the equality. Next we multiply (A 1*c*) by q, and using (A 1*b*), (A 3) and (A 4) leads to

$$\begin{aligned} q\frac{\partial q}{\partial t} &= h(u^+ - u^-)\, q - g\, p\, q - f \sum_{\ell=1}^{N} \mu_\ell \frac{\partial \xi_\ell}{\partial t}\, q + m\frac{\partial^2 p^2}{\partial t^2}\, q - n\ |q|\ q^2, \\ &= h(u^+ - u^-)\, q - g\, p\frac{\partial p}{\partial t} - \frac{\pi}{2} f \sum_{\ell=1}^{N} \mu_\ell \left(\frac{\partial \xi_\ell}{\partial t} + \theta_\ell^2\, \xi_\ell\right) \frac{\partial \xi_\ell}{\partial t} + m\frac{\partial}{\partial t}(p\, q^2) - nq^2\left(|q| - \frac{m}{n} q\right). \end{aligned} \tag{A 5}$$

Therefore we get

$$\begin{aligned}(u^+ - u^-)q &= \frac{1}{2}\frac{\partial}{\partial t}\left(\frac{g}{h}p^2 + \frac{1}{h}(1-2\,m\,p)\,q^2 + \frac{\pi}{2}\frac{f}{h}\sum_{\ell=1}^{N}\mu_\ell\,\theta_\ell^2\,\xi_\ell^2\right)\\ &\quad + \frac{\pi}{2}\frac{f}{h}\sum_{\ell=1}^{N}\mu_\ell\left(\frac{\partial \xi_\ell}{\partial t}\right)^2 + \frac{n}{h}\,q^2\left(|q| - \frac{m}{n}q\right).\end{aligned} \tag{A 6}$$

Besides, (A 1*a*) is multiplied by $u^\pm$ and integrated in space. After summation and integration by parts (the data are compactly supported), we get

$$\begin{aligned}\int_{\mathbb{R}}\left(u^+\frac{\partial u^+}{\partial t} + u^-\frac{\partial u^-}{\partial t}\right)dx &= -\int_{\mathbb{R}}\frac{c}{a}\sum_{\ell=1}^{N}\mu_\ell\left(u^+\frac{\partial \varphi_\ell^+}{\partial t} + u^-\frac{\partial \varphi_\ell^-}{\partial t}\right)dx\\ &\quad -\int_{\mathbb{R}} d\left(\left(\frac{\partial u^+}{\partial x}\right)^2 + \left(\frac{\partial u^-}{\partial x}\right)^2\right)dx - \int_{\mathbb{R}} e\,(u^+ - u^-)\,q\,dx.\end{aligned} \tag{A 7}$$

Thanks to the relations (A 2) and (A 6), the previous equation is simplified and the conclusion follows. □

B. Elimination of fractional derivatives

Here we prove that (2.23) can be approximated by (2.30). To simplify the proof, we consider the homogenized version (2.29*a*) of (2.23*a*)-(2.23*b*), we also restrict to a right-way propagation and lastly we note $u = u^+$ and $p = p^+$:

$$\frac{\partial u}{\partial t} + \frac{\partial}{\partial x}\left(au + b\frac{u^2}{2}\right) - \bar{c}\frac{\partial^{-1/2}}{\partial t^{-1/2}}\frac{\partial u}{\partial x} - d\frac{\partial^2 u}{\partial x^2} = -\bar{e}(1-2mp)\frac{\partial p}{\partial t}. \tag{A 1}$$

All the coefficients are defined in (2.4), (2.18), (2.25) and (2.27).

The first step is to write (A 1) in a dimensionless form. For a source signal of central frequency f_0, we define the characteristic wavelength $\lambda = a_0/f_0$. Then we introduce the non-dimensional quantities, indexed by a tilde: $x = \lambda\tilde{x}$, $t = \tilde{t}/f_0$, $u = u_0\tilde{u}$ and $p = p_0\tilde{p}$ where u_0 is the characteristic velocity, that will be determined later. We get:

$$\frac{\partial \tilde{u}}{\partial \tilde{t}} + \frac{\partial}{\partial \tilde{x}}\left(\tilde{u} + \tilde{b}\frac{\tilde{u}^2}{2}\right) - \tilde{c}\frac{\partial^{-1/2}}{\partial \tilde{t}^{-1/2}}\frac{\partial \tilde{u}}{\partial \tilde{x}} - \tilde{d}\frac{\partial^2 \tilde{u}}{\partial \tilde{x}^2} = -\tilde{e}(1-2\tilde{m}\tilde{p})\frac{\partial \tilde{p}}{\partial \tilde{t}}, \tag{A 2}$$

with

$$\tilde{b} = Mb = M\frac{\gamma+1}{2}, \quad \tilde{c} = \frac{\bar{c}}{a_0}\sqrt{\frac{\lambda}{a_0}}, \quad \tilde{d} = \frac{d}{a_0\lambda}, \quad \tilde{e} = \frac{\bar{e}p_0}{u_0} = \frac{V}{2AD\gamma M}, \quad \tilde{m} = mp_0 = \frac{\gamma-1}{2\gamma}. \tag{A 3}$$

$M = u_0/c_0$ is the characteristic Mach number. The typical value of M is obtained by equalizing $\tilde{b}$ and $\tilde{e}$:

$$\tilde{b} = \tilde{e} \Leftrightarrow M = \sqrt{\frac{V}{AD\gamma(\gamma+1)}}. \tag{A 4}$$

To find an approximation of (A 2), we introduce $\varepsilon = \max(\tilde{b}, \tilde{c}, \tilde{d}, \tilde{e})$ and we suppose that it is a small parameter. Then we define new quantities, defined with hats, by the relation $v = \varepsilon\hat{v}$, with $v = b$, c, d or e, such that all the quantities with a hat are at most equal to one. Then, starting from

(A 2), we get:

$$\begin{aligned}
\frac{\partial \tilde{u}}{\partial \tilde{x}} &= -\frac{\partial \tilde{u}}{\partial \tilde{t}} - \varepsilon \hat{b}\tilde{u}\frac{\partial \tilde{u}}{\partial \tilde{x}} + \varepsilon \hat{d}\frac{\partial^2 \tilde{u}}{\partial \tilde{x}^2} - \varepsilon \hat{e}(1-2\tilde{m}\tilde{p})\frac{\partial \tilde{p}}{\partial \tilde{t}} + \varepsilon \hat{c}\frac{\partial^{-1/2}}{\partial \tilde{t}^{-1/2}}\frac{\partial \tilde{u}}{\partial \tilde{x}}, \\
&= -\frac{\partial \tilde{u}}{\partial \tilde{t}} - \varepsilon \hat{b}\tilde{u}\frac{\partial \tilde{u}}{\partial \tilde{x}} + \varepsilon \hat{d}\frac{\partial^2 \tilde{u}}{\partial \tilde{x}^2} - \varepsilon \hat{e}(1-2\tilde{m}\tilde{p})\frac{\partial \tilde{p}}{\partial \tilde{t}} \\
&+ \varepsilon \hat{c}\frac{\partial^{-1/2}}{\partial \tilde{t}^{-1/2}}\left(-\frac{\partial \tilde{u}}{\partial \tilde{t}} - \varepsilon \hat{b}\tilde{u}\frac{\partial \tilde{u}}{\partial \tilde{x}} + \varepsilon \hat{d}\frac{\partial^2 \tilde{u}}{\partial \tilde{x}^2} - \varepsilon \hat{e}(1-2\tilde{m}\tilde{p})\frac{\partial \tilde{p}}{\partial \tilde{t}} + \varepsilon \hat{c}\frac{\partial^{-1/2}}{\partial \tilde{t}^{-1/2}}\frac{\partial \tilde{u}}{\partial \tilde{x}}\right), \\
&= -\frac{\partial \tilde{u}}{\partial \tilde{t}} - \varepsilon \hat{b}\tilde{u}\frac{\partial \tilde{u}}{\partial \tilde{x}} + \varepsilon \hat{d}\frac{\partial^2 \tilde{u}}{\partial \tilde{x}^2} - \varepsilon \hat{e}(1-2\tilde{m}\tilde{p})\frac{\partial \tilde{p}}{\partial \tilde{t}} - \varepsilon \hat{c}\frac{\partial^{1/2}\tilde{u}}{\partial \tilde{t}^{1/2}} + O(\varepsilon^2),
\end{aligned}$$

where we have used

$$\frac{\partial^{1/2}\tilde{u}}{\partial \tilde{t}^{1/2}} = \frac{\partial^{-1/2}}{\partial \tilde{t}^{-1/2}}\frac{\partial \tilde{u}}{\partial \tilde{t}}.$$

Therefore (A 2) can be approximated by:

$$\frac{\partial \tilde{u}}{\partial \tilde{t}} + \frac{\partial}{\partial \tilde{x}}\left(\tilde{u} + \tilde{b}\frac{\tilde{u}^2}{2}\right) - \tilde{c}\frac{\partial^{1/2}\tilde{u}}{\partial \tilde{t}^{1/2}} - \tilde{d}\frac{\partial^2 \tilde{u}}{\partial \tilde{x}^2} = -\tilde{e}(1-2\tilde{m}\tilde{p})\frac{\partial \tilde{p}}{\partial \tilde{t}}, \tag{A 5}$$

where neglected terms are small, of order ε^2. Using the values of Table (1), $M = 0.21$ is obtained from (A 4), in agreement with the experiments made in [43], for $f_0 = 500$ Hz. From this Mach value, we deduce finally

$$\tilde{b} = 0.22 = \tilde{e}, \quad \tilde{c} = 0.010, \quad \tilde{d} = 8.2410^{-8}, \quad \tilde{m} = 0.14. \tag{A 6}$$

Coming back to quantities with dimensions, the new model (2.30) is found. Note that in a dimensional form, (2.30*a*) and (2.23*a*)-(2.23*b*) are linked by the approximation

$$\frac{\partial u^{\pm}}{\partial t} \simeq \pm a\frac{\partial u^{\pm}}{\partial x}.$$

This is why $c(x)$ in (2.23*a*)-(2.23*b*) becomes $c(x)/a$ in (2.30*a*).

References

1. P. G. Kevrekidis, *Nonlinear waves in lattices: past, present, future*, IMA J. Appl. Math., **76**(3) (2011), 389-423.
2. N. Lazarides, M. Eleftheriou, G. P. Tsironis, *Discrete breathers in nonlinear magnetic metamaterials*, Phys. Rev. Lett., **97**(15) (2006), 157406.
3. N. Boechler, G. Theocharis, S. Job, P. G. Kevrekidis, M. A. Porter, C. Daraio, *Discrete breathers in one-dimensional diatomic granular crystals*, Phys. Rev. Lett., **104**(24) (2010), 244302.
4. B. F. Feng, T. Kawahara, *Discrete breathers in two-dimensional nonlinear lattices*, Wave Motion, **45**(2) (2007), 68-82.
5. M. Grabowski, P. Hawrylak, *Wave propagation in a nonlinear periodic medium*, Phys. Rev. B, **41**(9) (1990), 5783-5791.
6. Y. Wan, C. M. Soukoulis, *One-dimensional nonlinear Schrödinger equation: A nonlinear dynamical approach*, Phys. Rev. A, **41**(2) (1990), 800-809.
7. Y. Wan, C. M. Soukoulis, *Wave transmission in one-dimensional nonlinear lattice : multi stability and noise*, Springer Proceedings in Physics: Disorder and Nonlinearity, **39**, Springer-Verlag, Berlin (1989).
8. P. Hawrylak, M. Grabowski, *Self-induced gaps and optical bistability in semiconductor superlattices*, Phys. Rev. B, **40**(11) (1989), 8013-8016.
9. Q. Li, C. T. Chan, K. M. Ho, C. M. Soukoulis, *Wave propagation in nonlinear photonic band-gap materials*, Phys. Rev. B, **53**(23) (1996), 1577-1585.
10. Q. Li, C. M. Soukoulis, S. Pnevmatikos, E. N. Economou, *Scattering properties of solitons in nonlinear disordered chains*, Phys. Rev. B, **38**(16) (1988), 11888-11891.

11. Q. Li, S. Pnevmatikos, E. N. Economou, C. M. Soukoulis, *Lattice-soliton scattering in nonlinear atomic chains*, Phys. Rev. B, **37**(7) (1988), 3534-3541.
12. Y. V. Kartashov, B. A. Malomed, L. Torner, *Solitons in Nonlinear Lattices*, Rev. Mod. Phys., **83**(1) (2011), 247-305.
13. J. S. Russell, *Report on Waves, Made to the Meetings of the British Association in 1842-1843*, Report of the British Association for the Advancement of Science, John Murray, London (1844).
14. M. Remoissenet, *Waves Called Solitons: Concepts and Experiments*, Springer-Verlag, New-York (1999).
15. J. Engelbrecht, V. Fridman, E. Pelinovski, *Nonlinear Evolution Equations*, Longman, Harlow (1988).
16. T. Dauxois, M. Peyrard, *Physics of Solitons*, Cambridge University Press (2006).
17. J. Engelbrecht, A. Berezovski, A. Salupere, *Nonlinear deformation waves in solids and dispersion*, Wave Motion, **44** (2007), 493-500.
18. A. P. Chetverikov, W. Ebeling, M. G. Velarde, *Localized nonlinear, soliton-like waves in two-dimensional anharmonic lattices*, Wave Motion, **48** (2011), 753-760.
19. H. Y. Hao, H. J. Maris, *Experiments with acoustic solitons in crystalline solids*, Phys. Rev. B, **64**(6) (2001), 064302.
20. P. Hess, A.M. Lomonosov, *Solitary surface acoustic waves and bulk solitons in nanosecond and picosecond laser ultrasonics*, Ultrasonics, **50** (2010), 167-171.
21. S. V. Kuznetsov, *Soliton-like lamb waves*, J. Appl. Math. Mech., **73** (2009), 71-76.
22. A. M. Lomonosov, P. Hess, *Nonlinear surface acoustic waves: Realization of solitary pulses and fracture*, Ultrasonics, **48** (2008), 482-487.
23. A. P. Mayer, *Nonlinear surface acoustic waves: Theory*, Ultrasonics, **48** (2008), 478-481.
24. A. S Kovalev, A. P. Mayer, C. Eckl, G. A. Maugin, *Solitary Rayleigh waves in the presence of surface nonlinearities*, Phys. Rev. E, **66**(3) (2002), 036615.
25. M. de Billy, A. C. Hladky-Hennion, *On the formation of envelope solitons with tube ended by spherical beads*, Ultrasonics, **52** (2012), 851-860.
26. C. Daraio, V. F. Nesterenko, E. B. Herbold, S. Jin, *Tunability of solitary wave properties in one-dimensional strongly nonlinear phononic crystals*, Phys. Rev. E, **73**(2) (2006), 026610.
27. M. Moleron, A. Leonard, C. Daraio, *Solitary waves in chain of repelling magnets*, J. Appl. Phys., **115** (2014), 184901.
28. H. H. Dai, Y. Huo, *Solitary waves in an inhomogeneous rod composed of a general hyper elastic material*, Wave Motion, **35** (2002), 55-69.
29. K. R. Khusnutdinova, A. M. Samsonov, *Fission of longitudinal strain solitary wave in a delaminated bar*, Phys. Rev. E, **77**(6) (2008), 06603.
30. M. de Billy, A. C. Hladky-Hennion, *Generation of transversal envelope soliton in polymeric and wooden rods*, Ultrasonics, **54** (2014), 1281-1288.
31. D. R. Christie, K. J. Muirhead, R. H. Clarke, *Solitary waves in lower atmosphere*, Nature, **293** (1981), 46-49.
32. M. P. Rao, P. Castracane, S. Casadio, D. Fuà, G. Fiocco, *Observations of atmospheric solitary waves in the urban boundary layer*, Bound.-layer Meteor., **111** (2004), 85-108.
33. R. J. Doviak, S. S. Chen, D. R. Christie, *A thunderstorm-generated solitary wave observation compared with theory for nonlinear waves in a sheared atmosphere*, J. Atmos. Sci., **48**(1) (1991), 87-111.
34. C. E. Synolakis, *The run-up of solitary waves*, J. Fluid Mech., **185** (1987), 523-545.
35. Y. Li, F. Raichlen, *Non-breaking and breaking solitary wave run-up*, J. Fluid Mech., **456** (2002), 295-318.
36. J. R. Apel, L. A. Ostrovsky, Y. A. Stepanyants, J. F. Lynch, *Internal solitons in the ocean and their effect on underwater sound*, J. Acoust. Soc. Am., **121**(2) (2007), 695-722.
37. N. Sugimoto, M. Masuda, J. Ohno, D. Motoi, *Experimental demonstration of generation and propagation of acoustic solitary waves in a air-filled tube*, Phys. Rev. Lett., **83**(20) (1999), 4053-4056.
38. N. Sugimoto, *Propagation of nonlinear acoustic waves in a tunnel with an array of Helmholtz resonators*, J. Fluid. Mech., **244** (1992), 55-78.
39. N. Sugimoto, *Acoustic solitary waves in a tunnel with an array of Helmholtz resonators*, J. Acoust. Soc. Am., **99**(4) (1996), 1971-1976.
40. N. Sugimoto, M. Masuda, K. Yamashita, H. Horimoto, *Verification of acoustic solitary waves*, J. Fluid. Mech., **504** (2004), 271-299.
41. D. Matignon, *An introduction to fractional calculus*, Scaling, Fractals and Wavelets (Digital Signal and Image Processing Series), ISTE-Wiley, 2008.

42. L. Menguy, J. Gilbert, *Weakly nonlinear gas oscillations in air-filled tubes; solutions and experiments*, Acta Acustica united with Acustica, **86**(5) (2000), 798-810.
43. O. Richoux, B. Lombard, J. F. Mercier, *Generation of acoustic solitary waves in a lattice of Helmholtz resonators*, Wave Motion, **56** (2015), 85-99.
44. B. Lombard, J. F. Mercier, *Numerical modeling of nonlinear acoustic waves in a tube connected with Helmholtz resonators*, J. Comput. Phys., **259** (2014), 421-443.
45. B. Lombard, J.F. Mercier, O. Richoux, *Numerical investigation of acoustical solitons*, Proceedings of the Estonian Academy of Sciences, **64**(3) 304-310 (2015)
46. W. Chester, *Resonant oscillations in closed tubes*, J. Fluid Mech., **18** (1964), 44-64.
47. I. Podlubny, *Fractional Differential Equations*, Academic Press (1999).
48. P. Monkewitz, N. M. Nguyen-Vo, *The response of Helmholtz resonators to external excitation. Part 1. Single resonators*, J. Fluid Mech., **151** (1985), 477-497.
49. P. Monkewitz, *The response of Helmholtz resonators to external excitation. Part 2. Arrays of slit resonators*, J. Fluid Mech., **156** (1985), 151-166.
50. K. Diethelm, *An investigation of some nonclassical methods for the numerical approximation of Caputo-type fractional derivatives*, Numer. Algor., **47** (2008), 361-390.
51. E. F. Toro, *Riemann Solvers and Numerical Methods for Fluid Dynamics. A Practical Introduction*, Springer-Verlag (1999).
52. R. J. LeVeque, *Numerical methods for conservation laws*, 2nd edition, Birkhäuser-Verlag (1992).
53. J. P. Fouque, J. Garnier, G. Papanicolaou and K. Solna, *Wave propagation and time reversal in randomly layered media*, **56**, Springer Science and Business Media (2007) .